Non-hydrostatic model formulations for ultra-high resolution medium-range forecasting: compressible or anelastic ?

Nils Wedi, Pierre Benard, Karim Yessad, Sylvie Malardel
Mats Hamrud and George Mozdzynski

Many thanks to Agathe Untch and Fernando II

Outline

- Overview of the current status of non-hydrostatic modelling at ECMWF
- Identify main areas of concern and their suggested resolve
    - The spectral transform method
    - Compressible vs. unified hydrostatic-anelastic equations
- Conclusions

Introduction – A history

- **Resolution increases of the deterministic 10-day medium-range Integrated Forecast System (IFS) over ~25 years at ECMWF:**
  - **1987: T 106 (~125km)**
  - **1991: T 213 (~63km)**
  - **1998: T_L319 (~63km)**
  - **2000: T_L511 (~39km)**
  - **2006: T_L799 (~25km)**
  - **2010: T_L1279 (~16km)**
  - **2015?: T_L2047 (~10km)**
  - **2020-???: (~1-10km) Non-hydrostatic, cloud-permitting, substantially different cloud-microphysics and turbulence parametrization, substantially different dynamics-physics interaction ?**

Skewness and (excess) Kurtosis

Variance:

$$\sigma = \overline{(x-\overline{x})^2}$$

Skewness:

$$s = \frac{\overline{(x-\overline{x})^3}}{\sigma^{3/2}}$$

(excess) Kurtosis:

$$k = \frac{\overline{(x-\overline{x})^4}}{\sigma^2} - 3$$

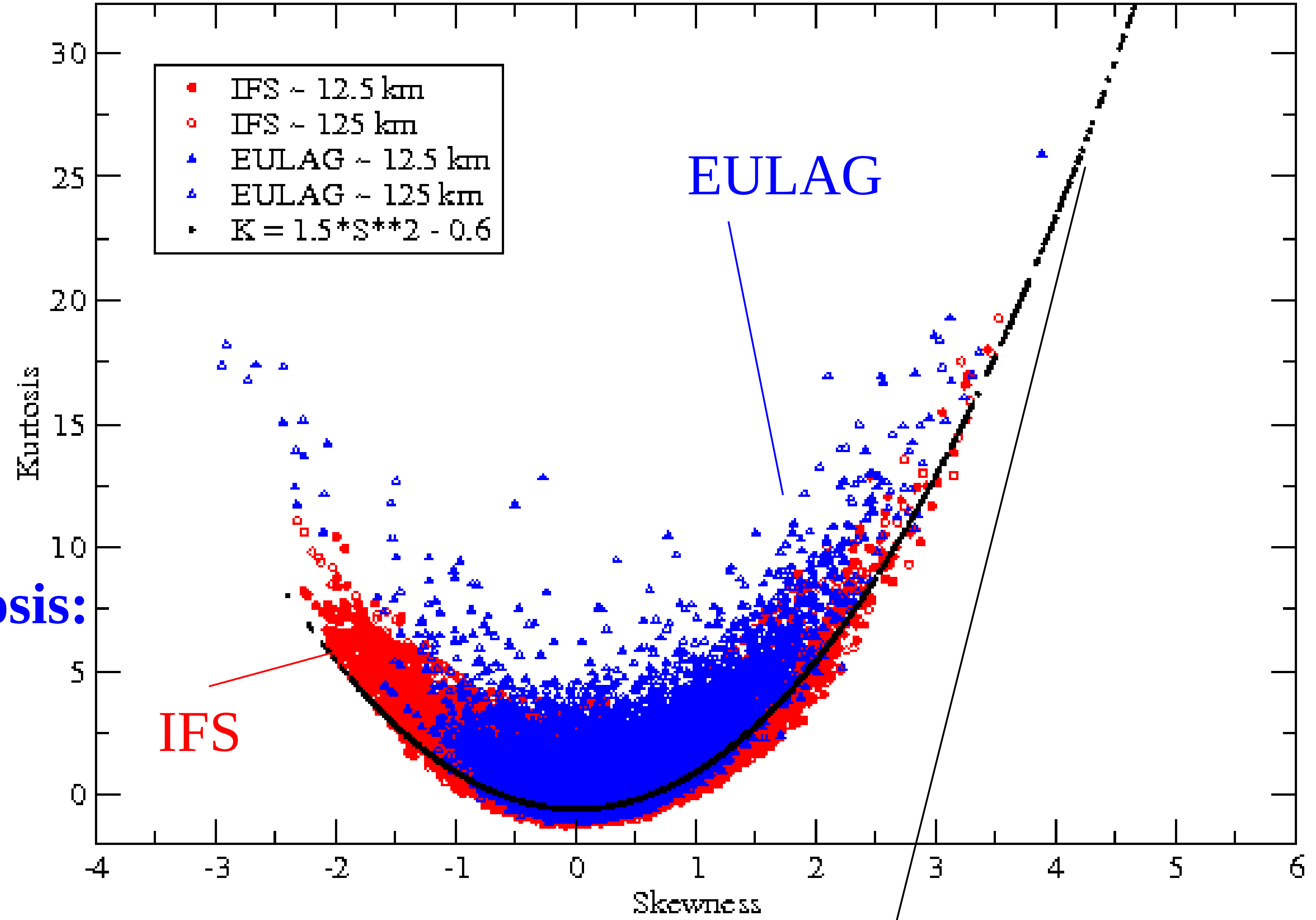

Predicted from linear stochastic models forced with non-Gaussian noise (Sardeshmukh and Surda, 2009)

Higher resolution influence (250hPa vorticity)

Variance:

$$\sigma = \overline{(x-\overline{x})^2}$$

Skewness:

$$s = \frac{\overline{(x-\overline{x})^3}}{\sigma^{3/2}}$$

Kurtosis:

$$k = \frac{\overline{(x-\overline{x})^4}}{\sigma^2} - 3$$

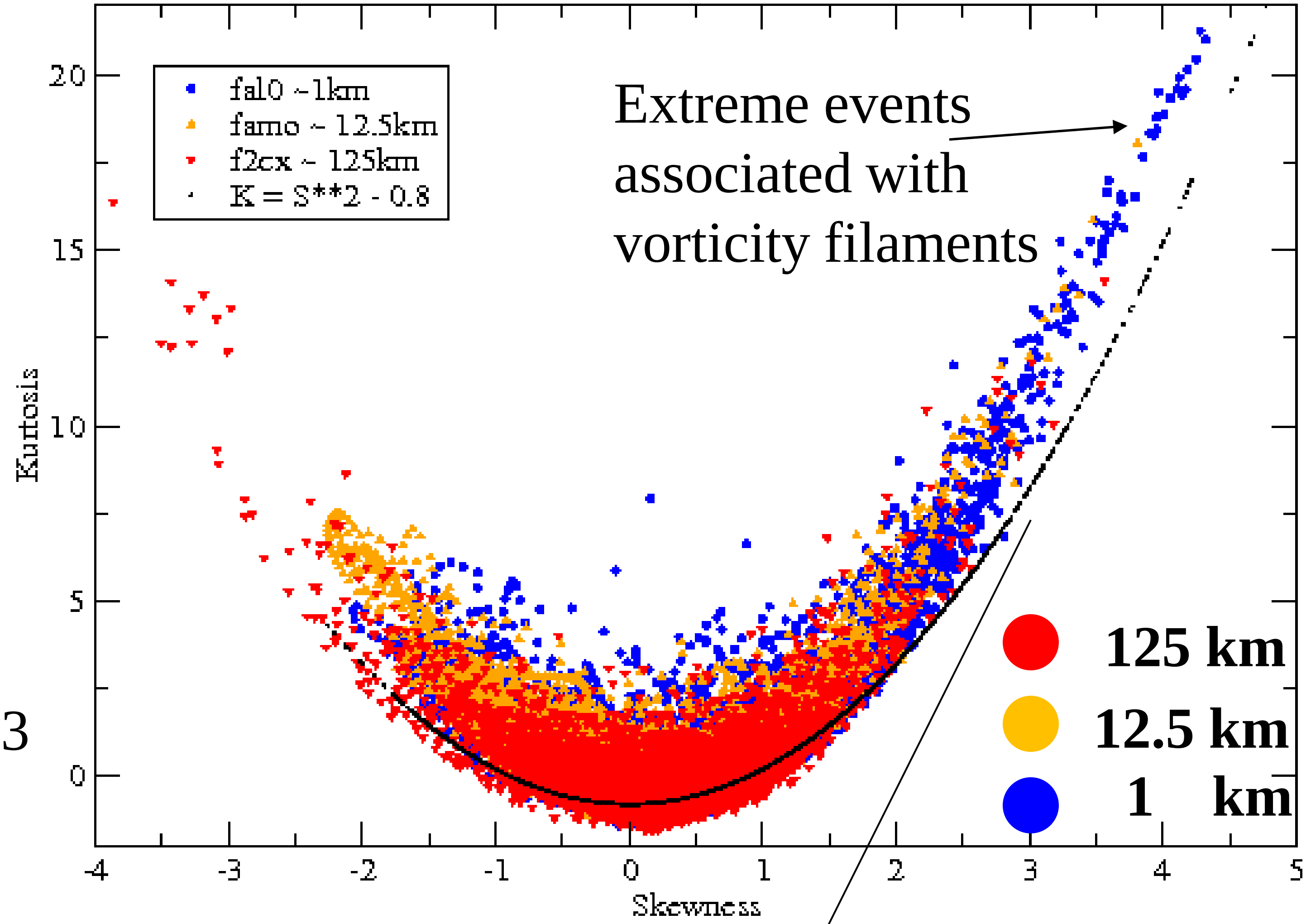

Predicted from linear stochastic models forced with non-Gaussian noise (Sardeshmukh and Surda, 2009)

Cyclonic vorticity (extreme events)

For example *vorticity filaments* are associated with high skewness and high (excess) kurtosis !

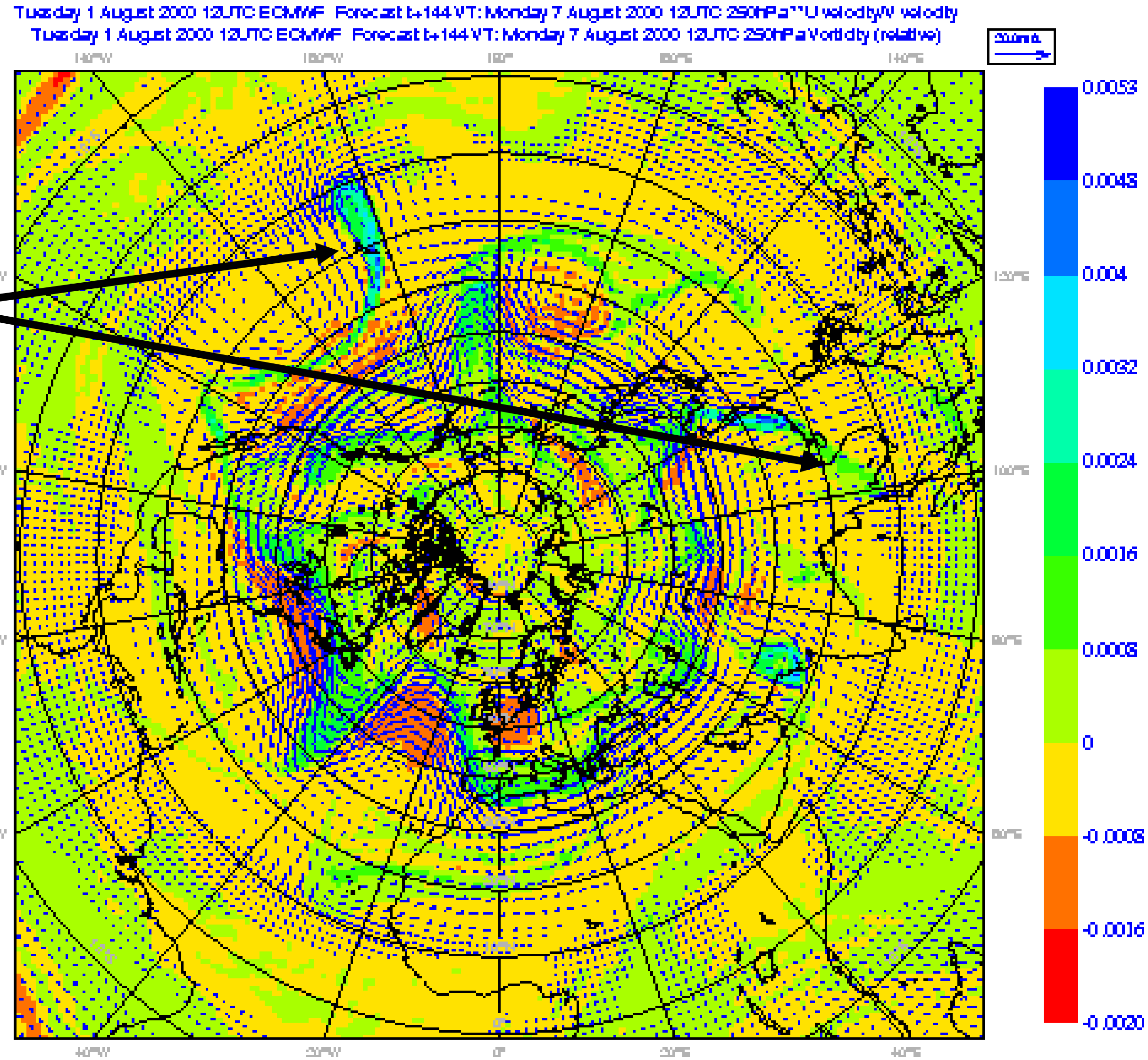

ECMWF

Ultra-high resolution global IFS simulations

- **T_L0799 (~ 25km) >> 843,490 points per field/level**
- **T_L1279 (~ 16km) >> 2,140,702 points per field/level**
- **T_L2047 (~ 10km) >> 5,447,118 points per field/level**
- **T_L3999 (~ 5km) >> 20,696,844 points per field/level (world record for spectral model ?!)**

Max global altitude = 6503m

Orography – T1279

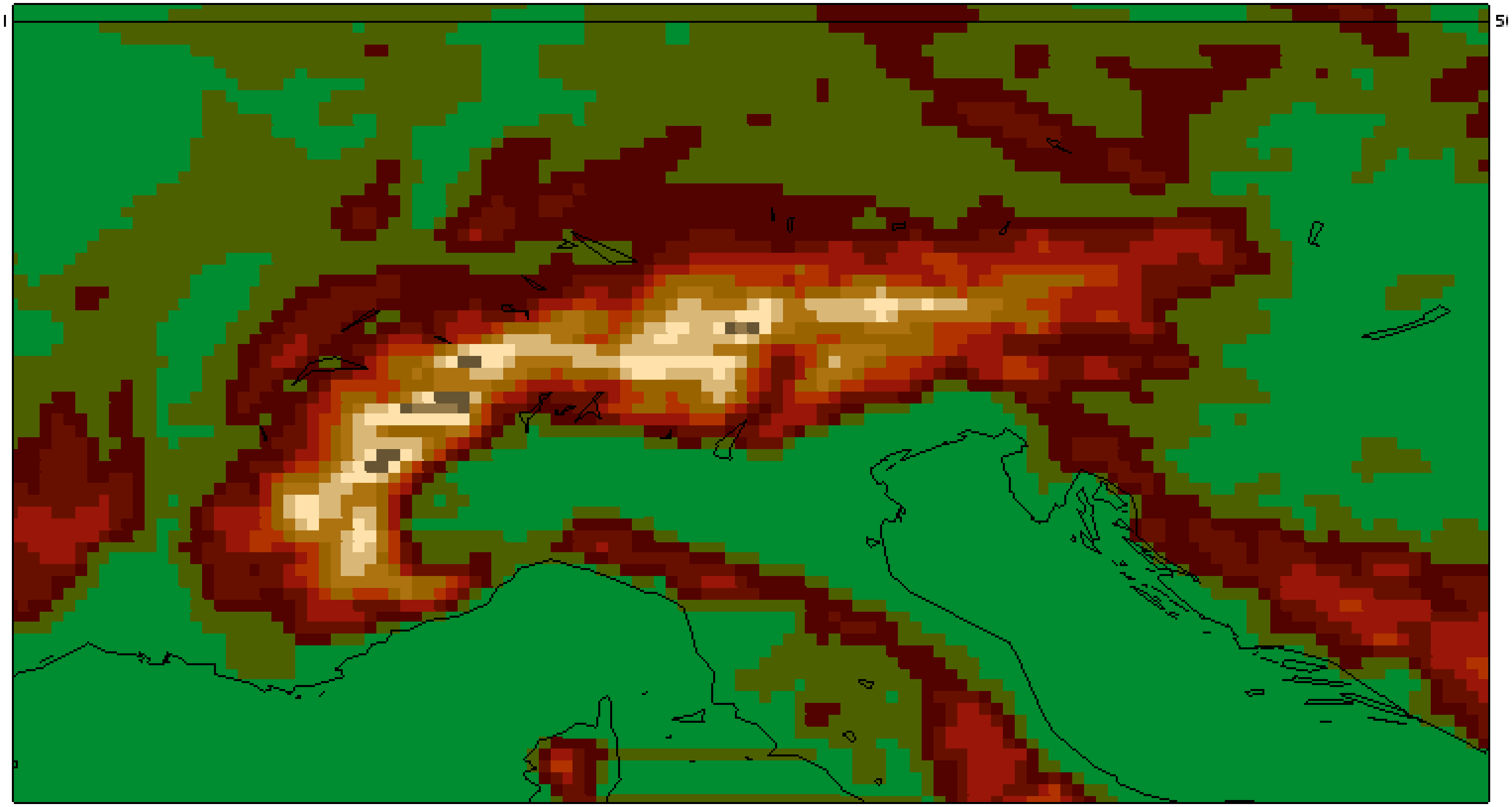

Alps

Orography - T3999

Max global altitude = 7185m

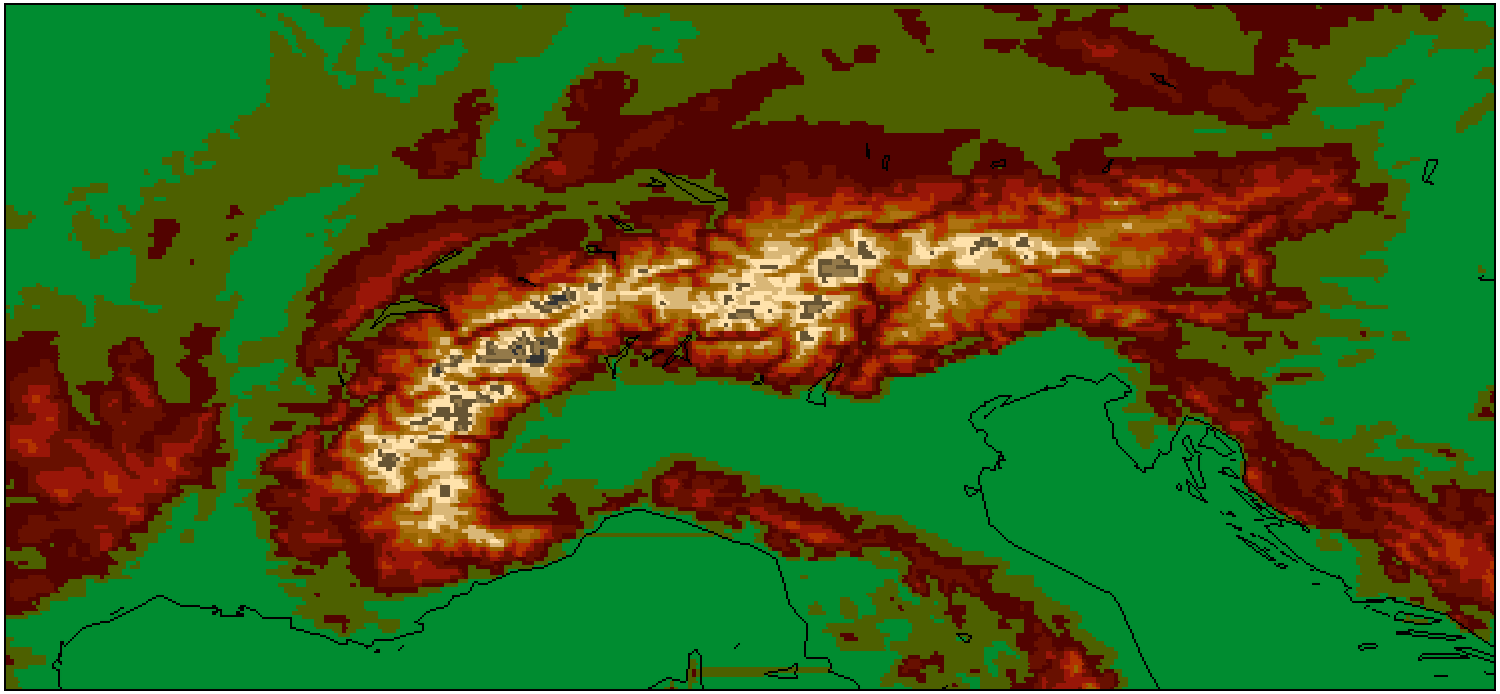

Alps

The Gaussian grid

About 30% reduction in number of points

Full grid

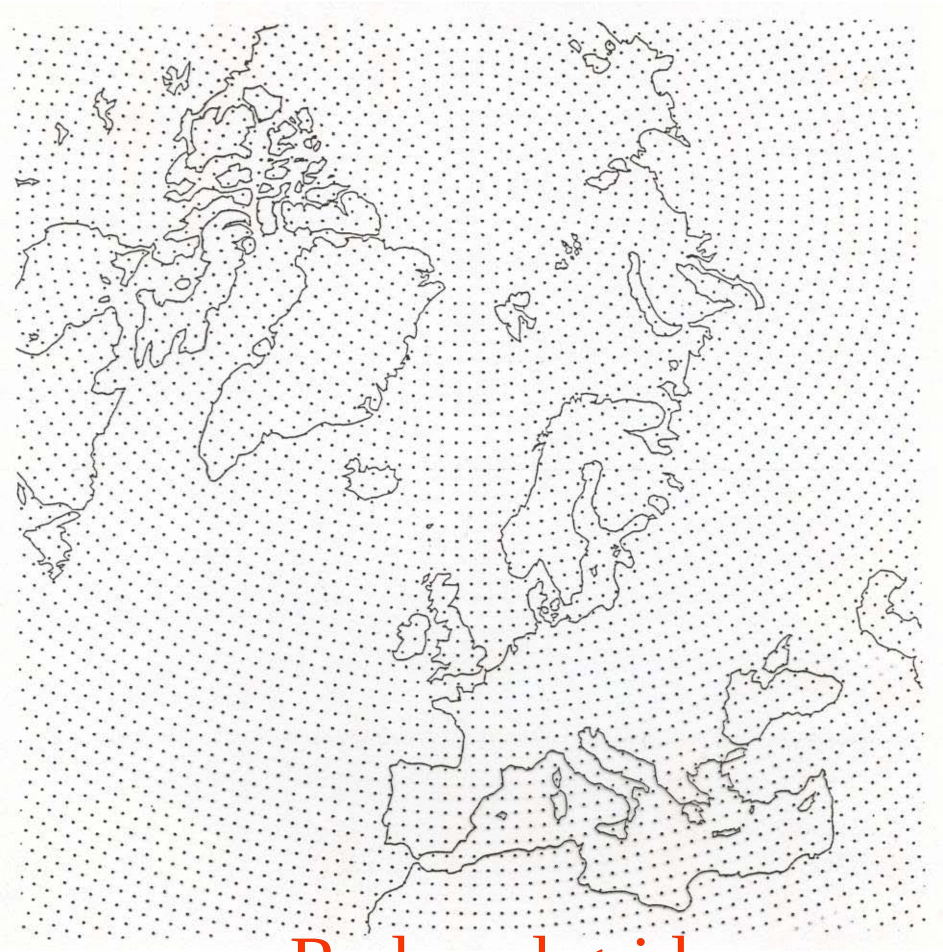

Reduced grid

Reduction in the number of Fourier points at high latitudes is possible because the associated Legendre functions are very small near the poles for large m.

ECMWF

Preparing for the future: The nonhydrostatic IFS

- **Developed by Météo-France and its ALADIN partners** ***Bubnová et al., (1995); ALADIN (1997); Bénard et al. (2004,2005,2010)***
- **Made available in IFS/Arpège by Météo-France** ***(Yessad, 2008)***
- **Testing of NH-IFS described in Techmemo TM594** ***(Wedi et al. 2009)***

Quasi two-dimensional orographic flow with linear vertical shear

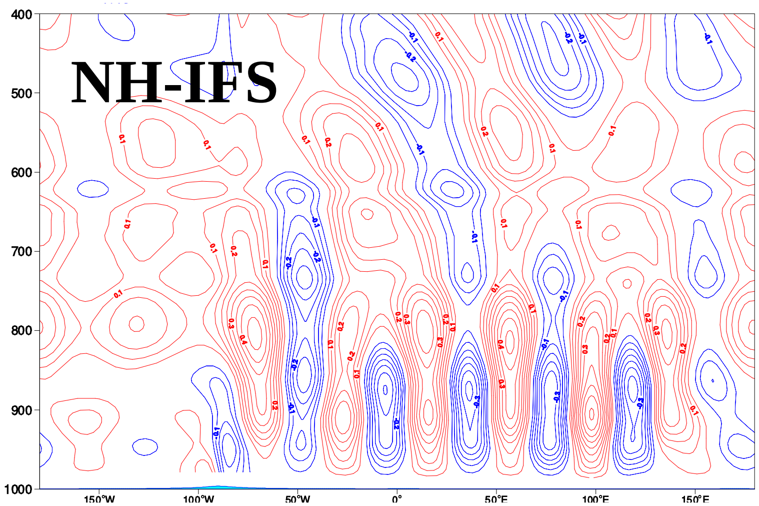

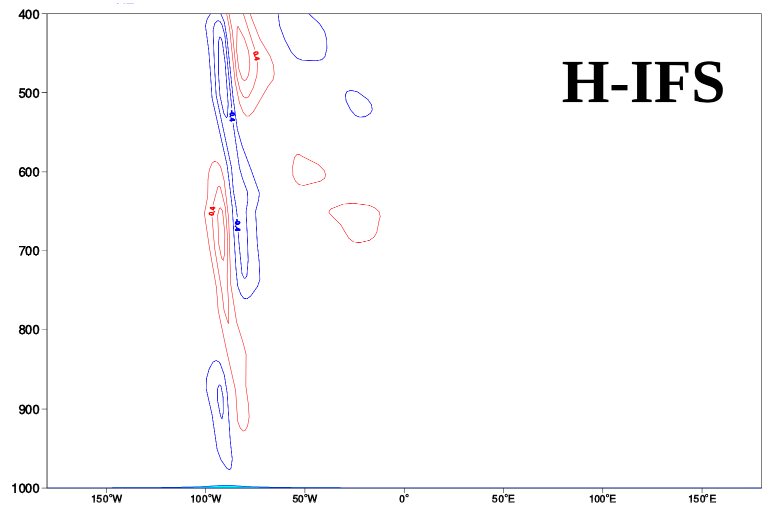

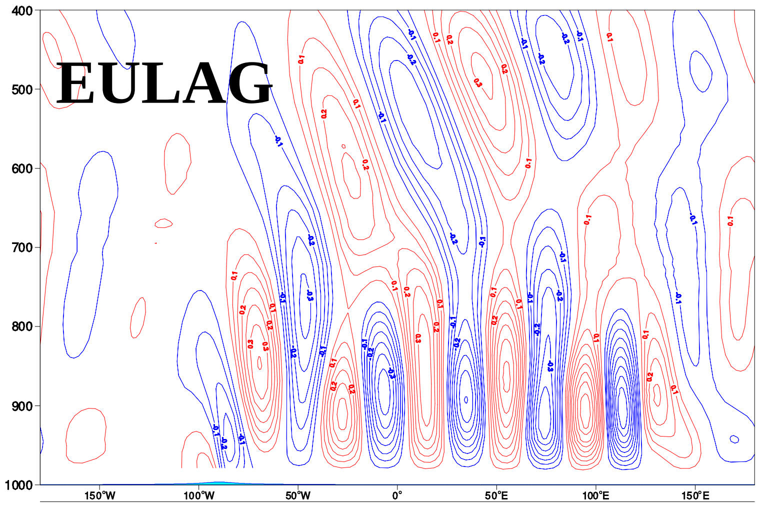

The figures illustrate the correct horizontal (NH) and the (incorrect) vertical (H) propagation of gravity waves in this case (Keller, 1994). Shown is vertical velocity.

(Wedi and Smolarkiewicz, 2009)

ECMWF

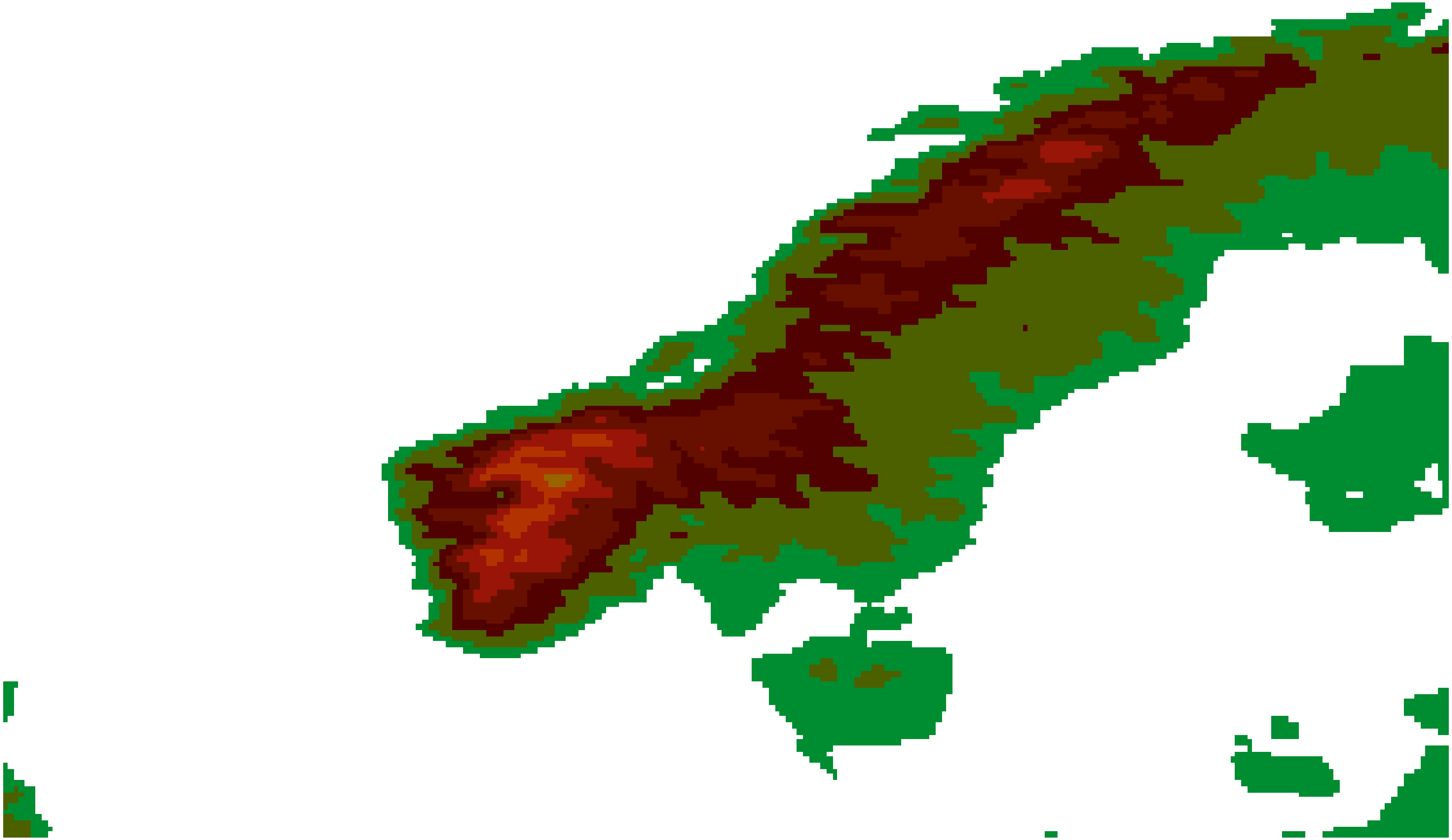

ECMWF

Orography – T1279

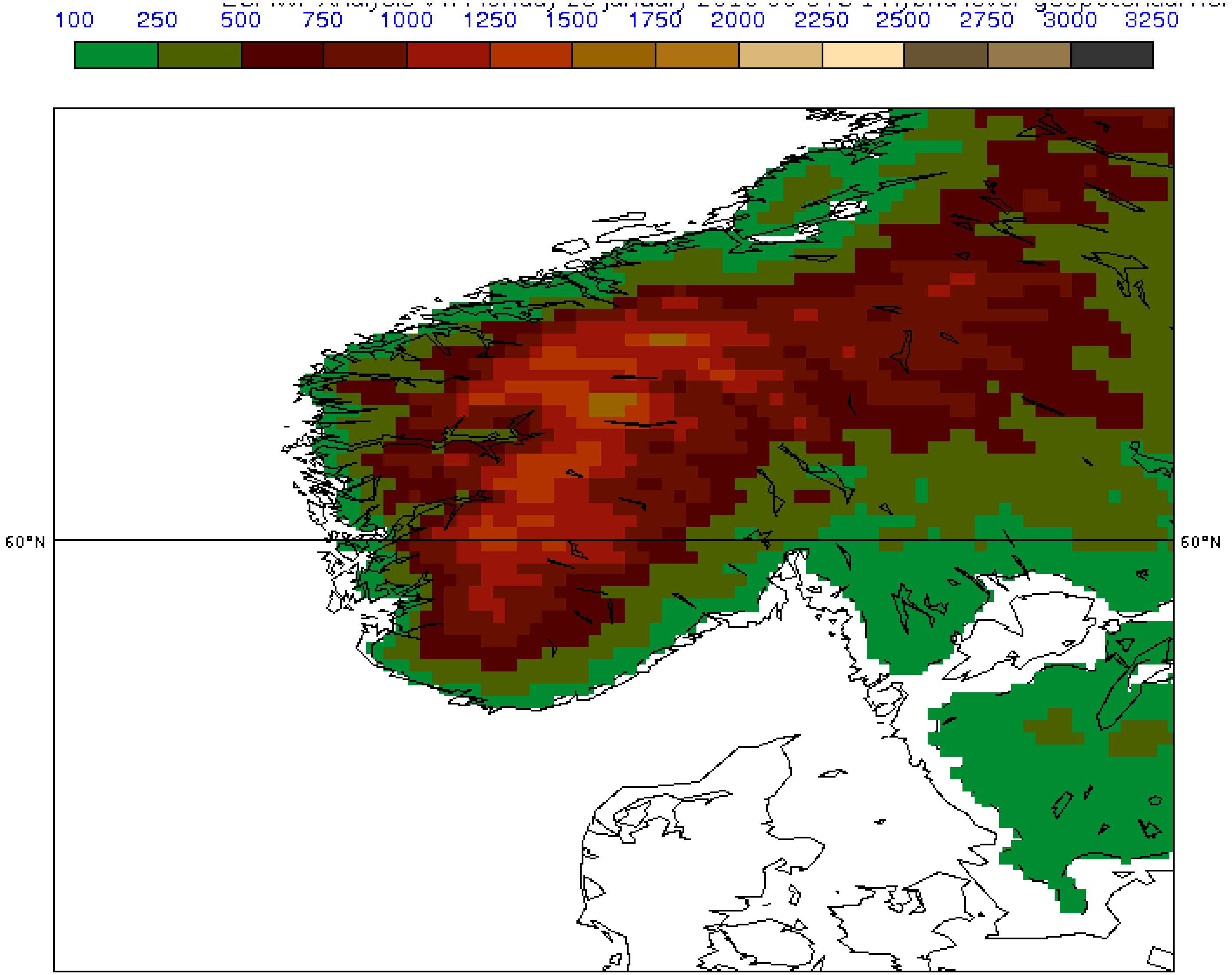

ECMWF

Orography T3999

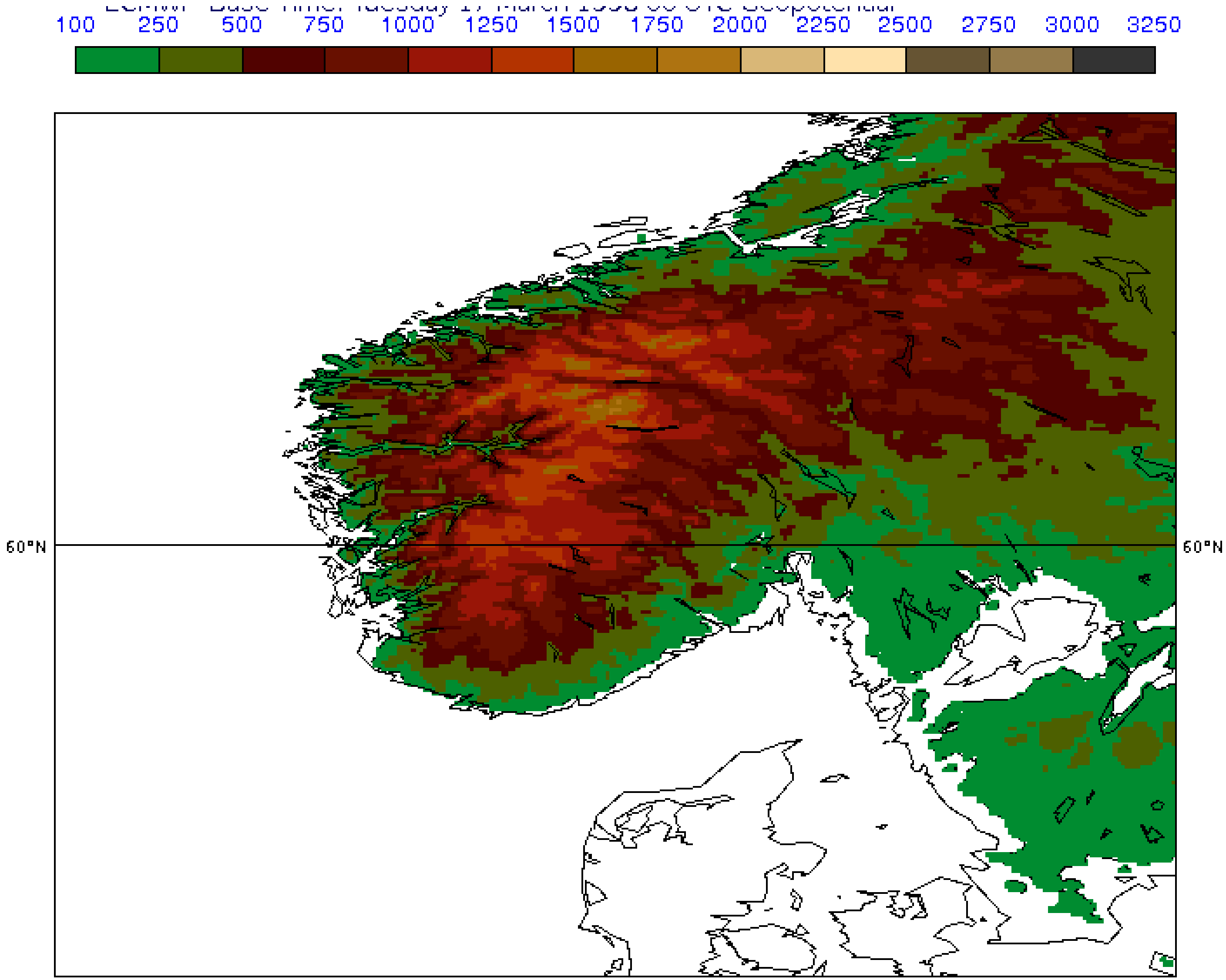

ECMWF

Cloud cover 24h forecast T3999 (~5km)

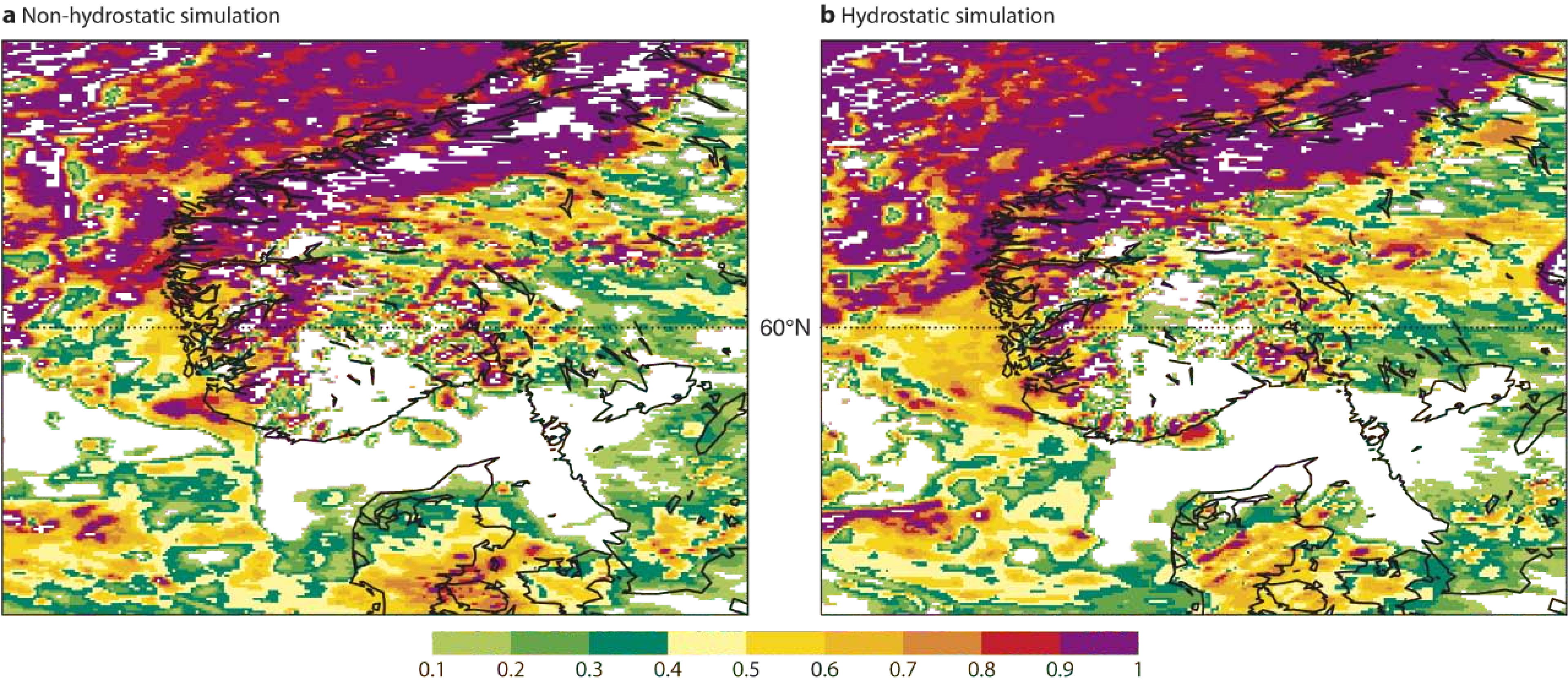

Era-Interim shows a wind shear with height in the troposphere over the region!

ECMWF

T1279 Precipitation

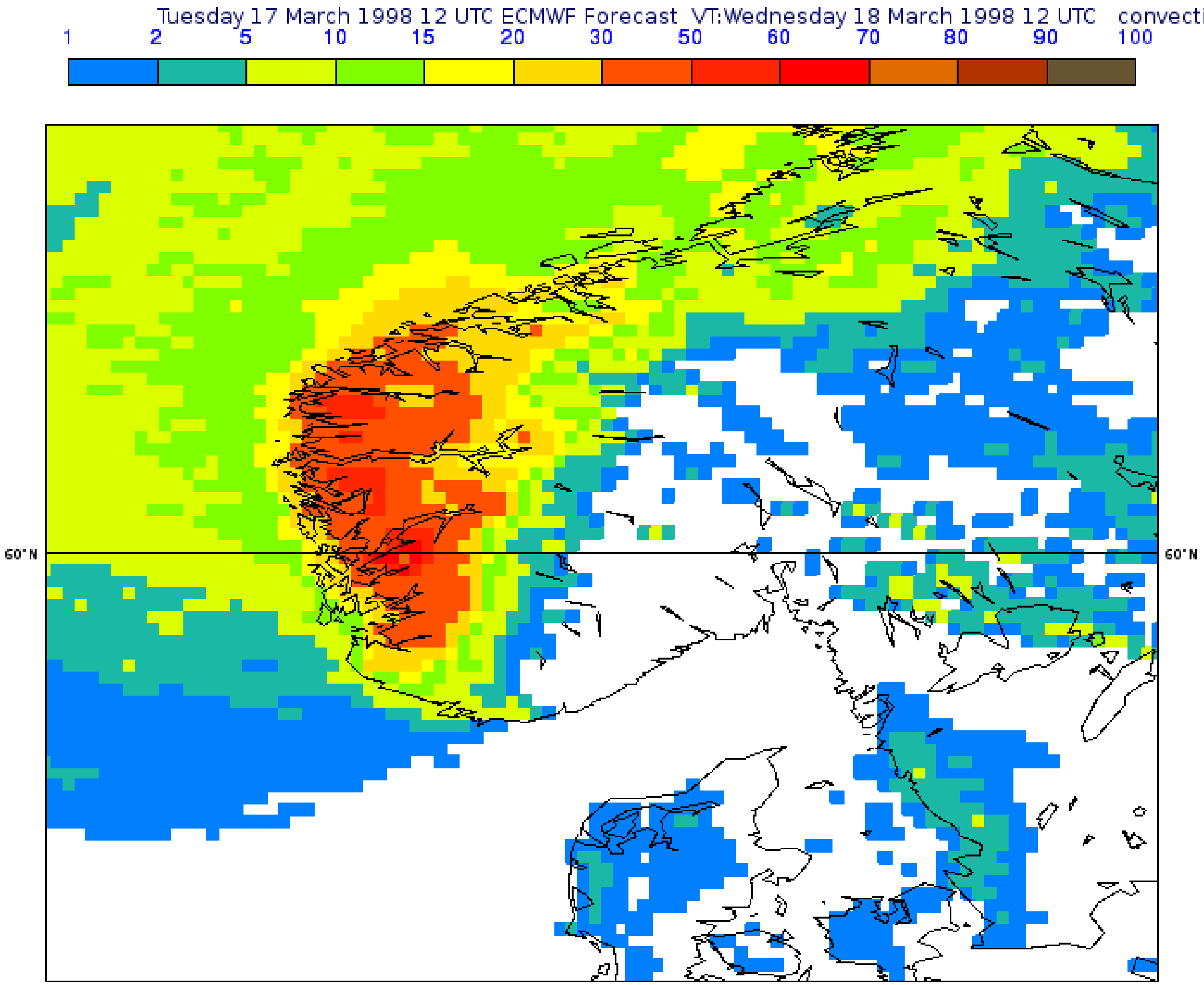

ECMWF

T3999 precipitation

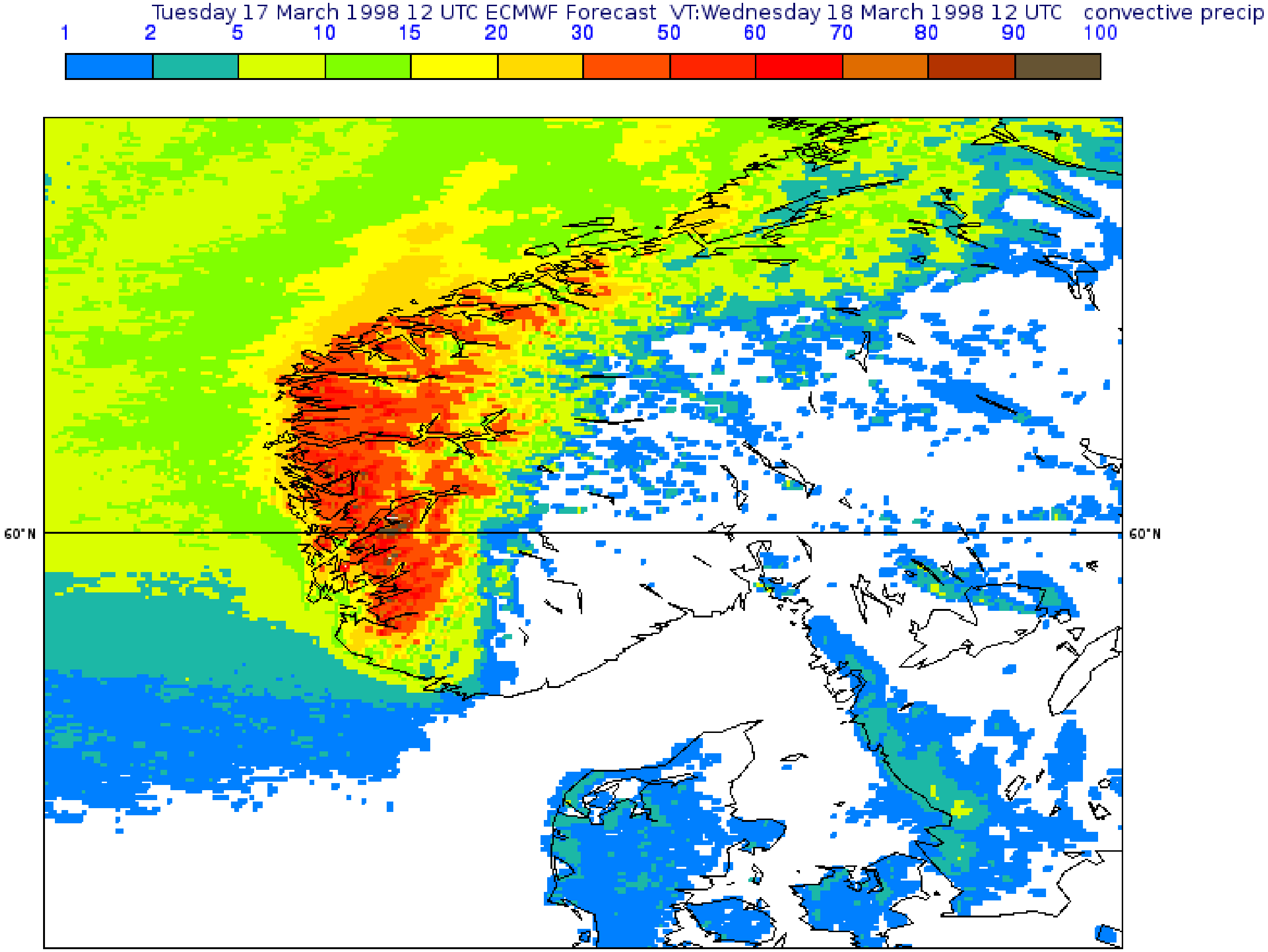

ECMWF

Computational Cost at T_L2047

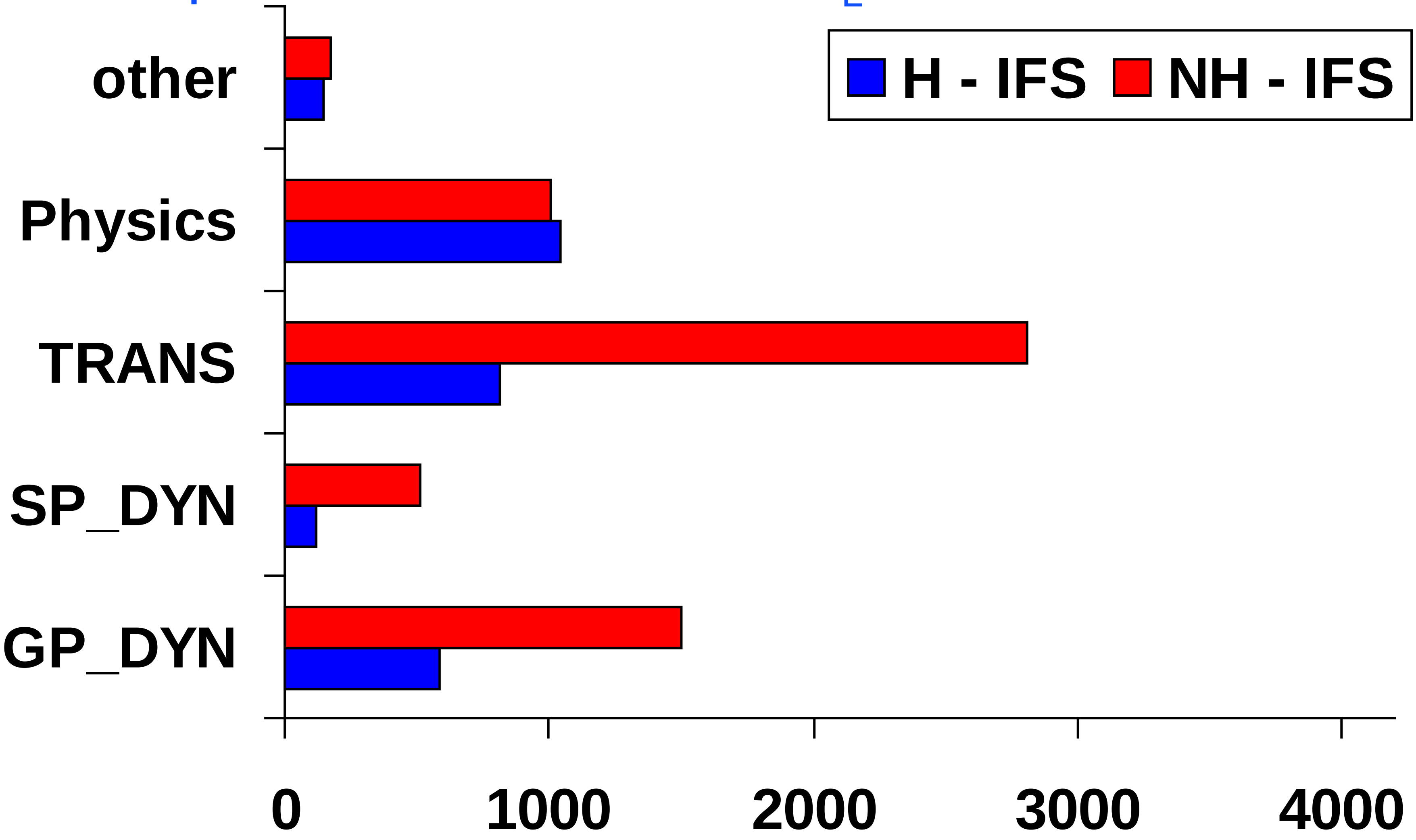

Total cost increase NH – H 106 %

Computational Cost at T_L3999

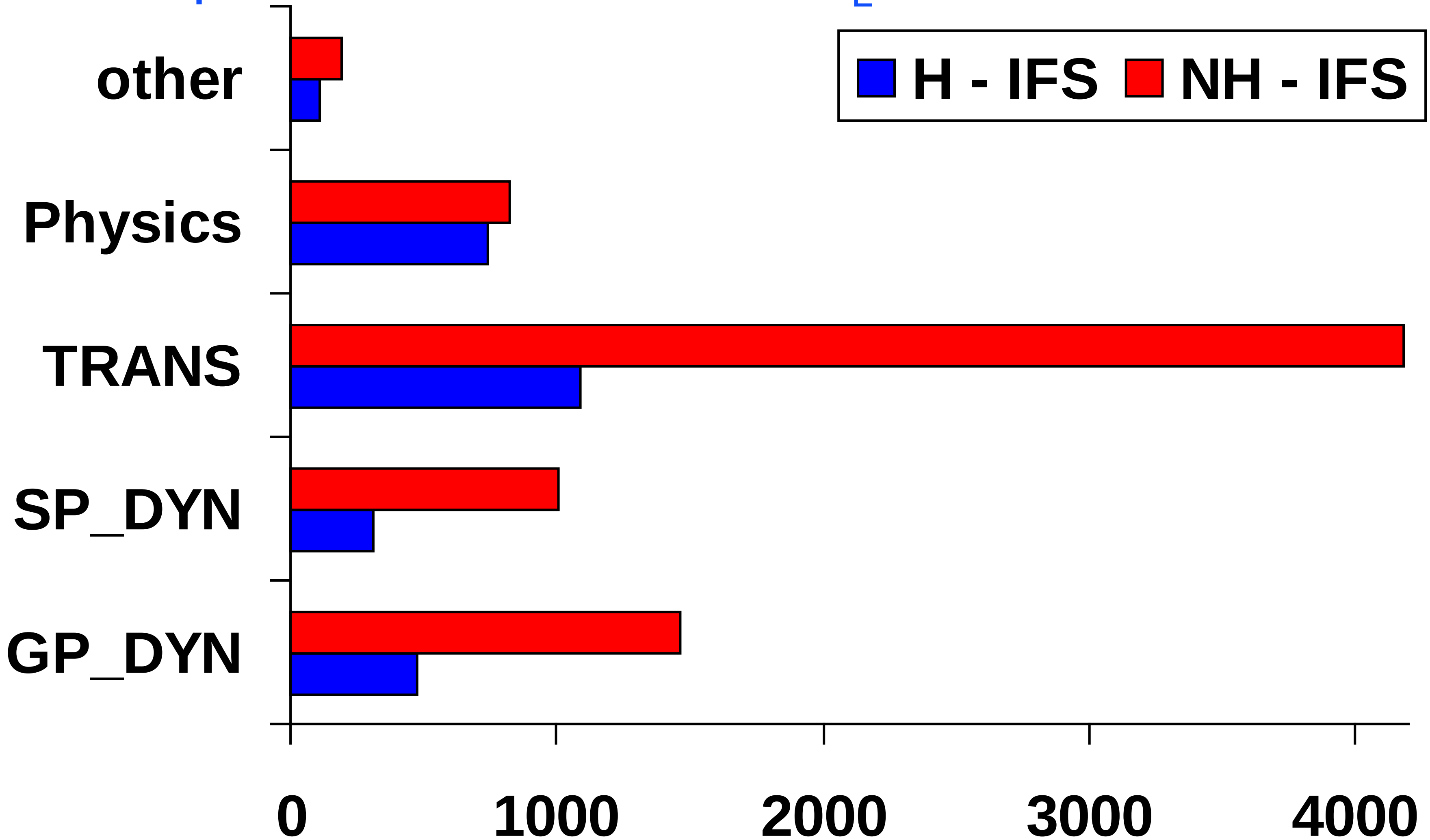

Total cost increase for 24h forecast: H 50min vs. NH 150min

ECMWF

Computational Cost at T_L3999 hydrostatic vs. non-hydrostatic IFS

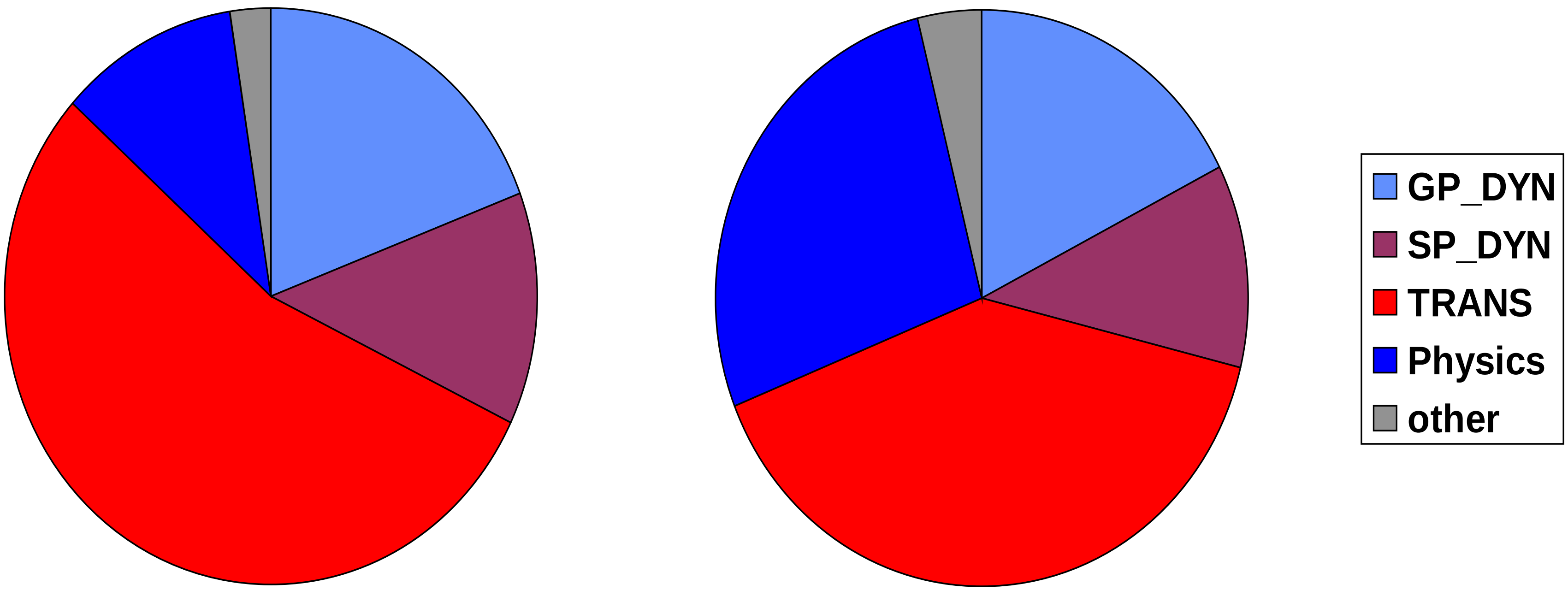

NH T_L3999 **H T_L3999**

ECMWF

The spectral transform method

Schematic description of the spectral transform method in the ECMWF IFS model

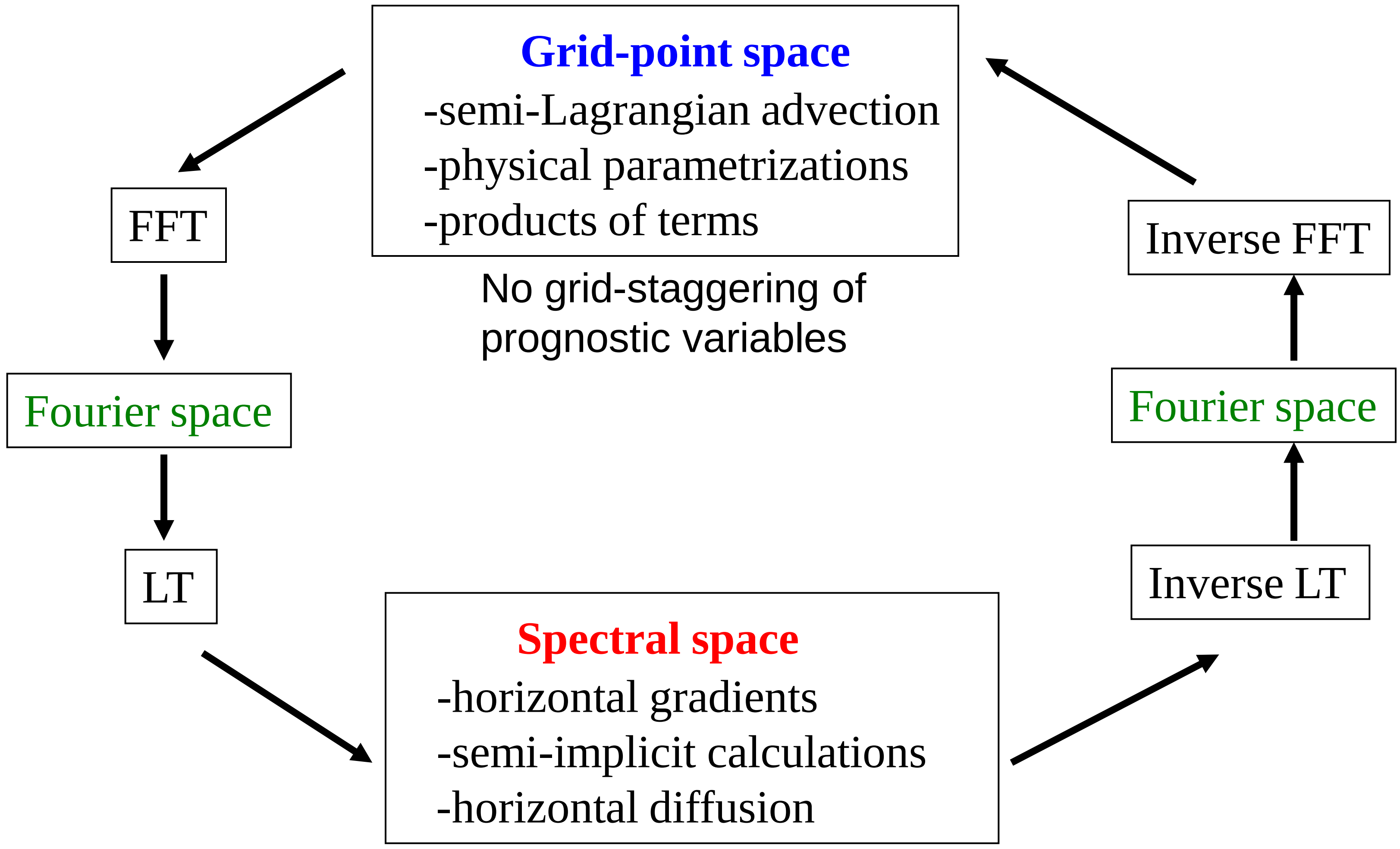

FFT: Fast Fourier Transform, LT: Legendre Transform

Horizontal discretisation of variable X (e.g. temperature)

$$X(\lambda,\mu,\eta,t) = \sum_{m=-N}^{N} \sum_{n=|m|}^{N} X_n^m(\eta,t) Y_n^m(\lambda,\mu)$$

Triangular truncation (isotropic)

Spherical harmonics

$$X_n^m(\eta,t) = \frac{1}{4\pi} \int_{-1}^{1} \int_{0}^{2\pi} X(\lambda,\mu,\eta,t) P_n^m(\mu) e^{-im\lambda} d\lambda\, d\mu$$

Fourier functions

associated Legendre polynomials

Legendre transform
by Gaussian quadrature
using $N_L \geq (2N+1)/2$
"Gaussian" latitudes (linear grid)
((3N+1)/2 if quadratic grid)
"fast" algorithm desirable …

FFT (fast Fourier transform)
using
$N_F \geq 2N+1$
points (linear grid)
(3N+1 if quadratic grid)
"fast" algorithm available …

Triangular truncation:

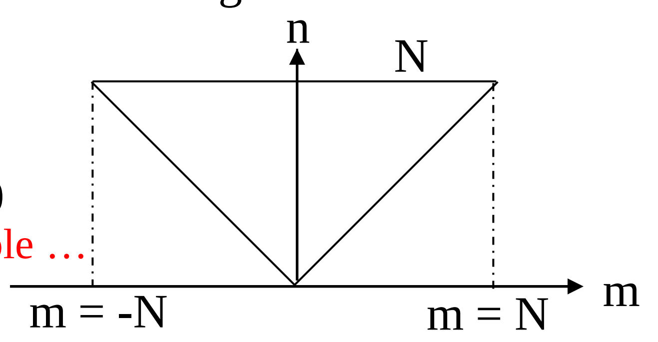

ECMWF

Computation of the associated Legendre polynomials

- **Increase of error due to recurrence formulae (Belousov, 1962)**
- **Recent changes to transform package went into cycle 35r3 that allow the computation of Legendre functions and Gaussian latitudes in double precision following *(Schwarztrauber, 2002)* and increased accuracy 10^{-13} instead of 10^{-12}.**
- **Note: the increased accuracy leads in the "*Courtier and Naughton* (1994) procedure for the reduced Gaussian grid" to slightly more points near the poles for all resolutions.**
- **Note: At resolutions > T3999 above procedure needs review!**

Spectral transform method

- **FFT can be computed as C*N*log(N) where C is a small positive number and N is the cut-off wave number in the triangular truncation.**
- **Ordinary Legendre transform is $O(N^2)$ but can be combined with the fields/levels such that the arising matrix-matrix multiplies make use of the highly optimized BLAS routine DGEMM.**
- **But overall cost is $O(N^3)$ for both memory and CPU time requirements.**

➡ **Desire to use a fast Legendre transform where the cost is proportional to C*N*log(N) with C << N**

and thus overall cost N^2*log(N)

Fast Legendre transform

- The algorithm proposed in *(Tygert, 2008)* suitably fits into the IFS transform library by simply replacing the single DGEMM call with 2 new steps plus more expensive pre-computations.
- (1) Instead of the recursive *Cuppen divide-and-conquer algorithm (Tygert, 2008)* we use the so called *butterfly algorithm (Tygert, 2010)* based on a matrix compression technique via rank reduction with a specified accuracy to accelerate the arising *matrix-vector multiplies (sub-problems still use dgemm).*
- (2) The arising interpolation from one set of roots of the associated Legendre polynomials to another can be accelerated by using a *FMM (fast multipole method).*

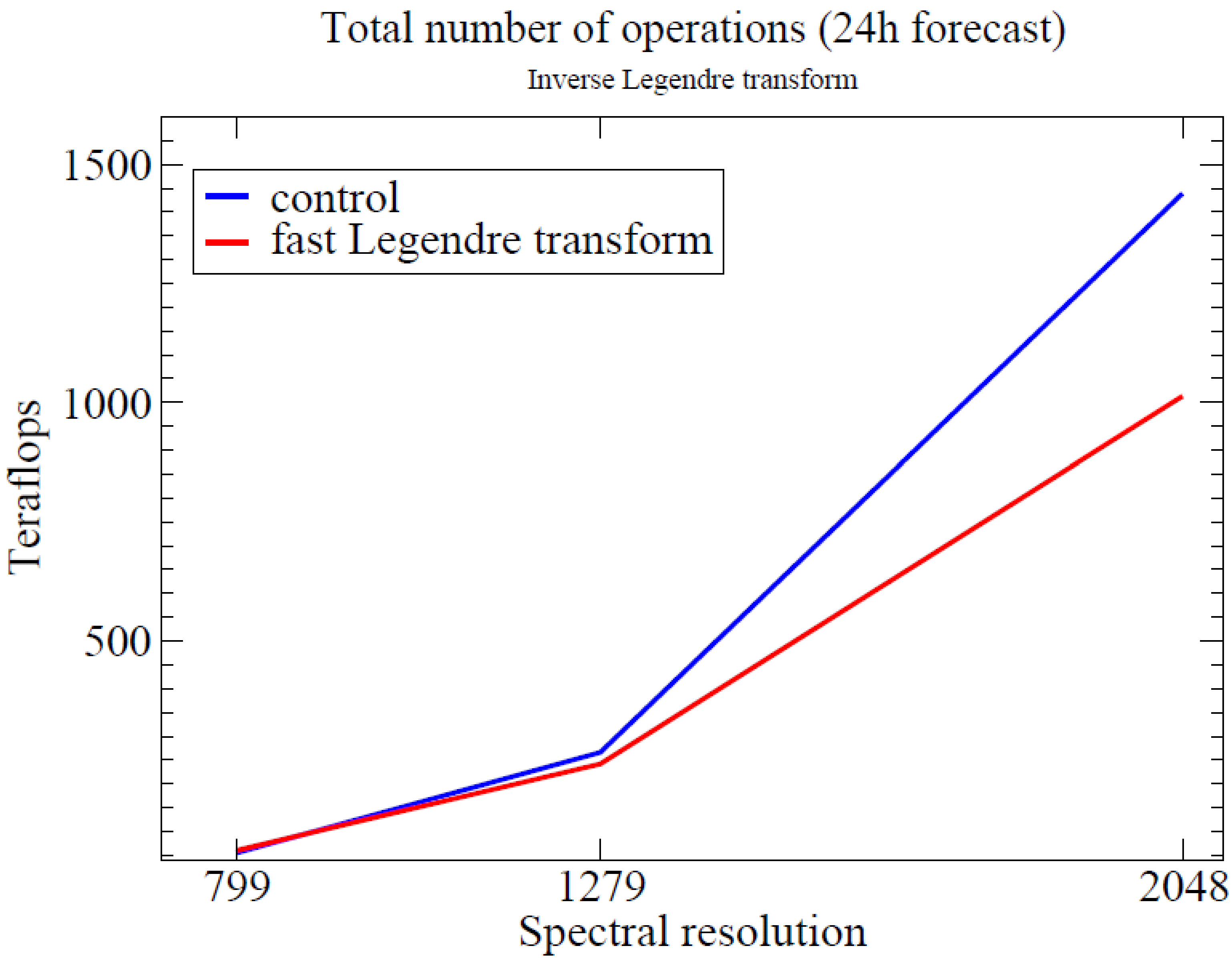
Total number of operations (24h forecast)
Inverse Legendre transform
control
fast Legendre transform
1500
1000
500
Teraflops
799
1279
2048
Spectral resolution

ECMWF

The IFS NH equations

Vertical coordinate

$$\pi = A(\eta) + B(\eta)\pi_s(\lambda, \phi, t)$$

hybrid vertical coordinate

Simmons and Burridge (1981)

Denotes hydrostatic pressure in the context of a shallow, vertically unbounded planetary atmosphere.

Prognostic surface pressure tendency:

$$\frac{\partial \pi_s}{\partial t} = -\int_0^1 \nabla_\eta \cdot (m\mathbf{v}_h) d\eta,$$

with $m \equiv \partial \pi / \partial \eta$

coordinate transformation coefficient

Two new prognostic variables in the nonhydrostatic formulation

$$\mathcal{Q} \equiv \log(p/\pi)$$

'Nonhydrostatic pressure departure'

$$d \equiv -g(p/mRT)\partial w/\partial \eta$$

'vertical divergence'

Define also: $\mathcal{D} \equiv d + \mathcal{X}$

With residual residual

$$\mathcal{X} \equiv (p/RTm)\nabla_\eta \Phi \cdot \partial \mathbf{v}_h/\partial \eta$$

Three-dimensional divergence writes

$$D_3 = \nabla_\eta \cdot \mathbf{v}_h + \mathcal{X} + d.$$

NH-IFS prognostic equations

$$\frac{d\mathbf{v}_h}{dt} = -\frac{RT}{p}\nabla_\eta p - \frac{1}{m}\frac{\partial p}{\partial \eta}\nabla_\eta \Phi - 2\Omega \times \mathbf{v}_h + P_{\mathbf{v}},$$

$$\frac{d\mathcal{D}}{dt} = \frac{dd}{dt} + \frac{d\mathcal{X}}{dt} = -\frac{gp}{mRT}\frac{\partial P_w}{\partial \eta},$$

$$\frac{dT}{dt} = -\frac{RT}{c_v}D_3 + \frac{c_p}{c_v}P_T,$$

$$\frac{d\mathcal{Q}}{dt} = -\frac{c_p}{c_v}D_3 - \frac{1}{\pi}\frac{d\pi}{dt} + \frac{c_p}{c_v T}P_T.$$

$$\frac{\partial \pi_s}{\partial t} = -\int_0^1 \nabla_\eta \cdot (m\mathbf{v}_h)d\eta,$$

'Physics'

Diagnostic relations

$$\frac{dd}{dt} = d(\nabla_\eta \cdot \mathbf{v}_h - D_3) - \frac{gp}{mRT}\left(\frac{\partial(dw/dt)}{\partial\eta} - \nabla_\eta w \cdot \frac{\partial \mathbf{v}_h}{\partial\eta}\right)$$

With

$$dw/dt = g\partial(p-\pi)/\partial\pi + P_w$$

Auxiliary diagnostic relations

$$
\begin{aligned}
\Phi &= \Phi_s + \int_\eta^1 \frac{mRT}{\pi} e^{-Q} d\eta, \\
m\frac{d\eta}{dt} &= B(\eta) \int_0^1 \nabla_\eta (m\mathbf{v}_h) d\eta - \int_0^\eta \nabla_\eta \cdot (m\mathbf{v}_h) d\eta, \\
\frac{d\pi}{dt} &= \mathbf{v}_h \cdot \nabla_\eta \pi - \int_0^\eta \nabla_\eta \cdot (m\mathbf{v}_h) d\eta, \\
\nabla_\eta (gw) &= \nabla_\eta (gw_s) + \int_\eta^1 \nabla_\eta \left(d\frac{mRT}{p} \right) d\eta, \\
w_s &= \mathbf{v}_{h,s} \cdot \nabla_\eta \Phi_s,
\end{aligned}
$$

Numerical solution

- Advection via a two-time-level semi-Lagrangian numerical technique as before.
- Semi-implicit procedure with two reference states with respect to gravity and acoustic waves, respectively.
- The resulting Helmholtz equation is more complicated than in the hydrostatic case but can still be solved (subject to some constraints on the vertical discretization) with a direct spectral method as before.

(Benard et al 2004,2005,2010)

Towards a unified hydrostatic-anelastic system

- **Scientifically, the benefit of having a prognostic equation for non-hydrostatic pressure departure is unclear.**
- **The coupling to the physics is ambiguous.**
- **For stability reasons, the NH system requires at least one iteration, which essentially doubles the number of spectral transforms.**
- **Given the cost of the spectral transforms, any reduction in the number of prognostic variables will save costs.**

Unapproximated Euler equations

$$\frac{d\mathbf{v}}{dt} = -\frac{1}{\rho}\nabla p - g\mathbf{k} + P_{\mathbf{v}},$$

$$\frac{1}{\rho}\frac{d\rho}{dt} = -\nabla \cdot \mathbf{v},$$

$$\frac{d\theta}{dt} = (\frac{\pi}{p_{00}})^{\kappa} P_T,$$

Unified system

(Arakawa and Konor, 2009)

presented here in the context of IFS

$$\rho_{qs} \equiv \frac{\pi}{R\tilde{T}}$$

$$\frac{\partial \pi}{\partial z} \equiv -\rho_{qs} g$$

$$\frac{1}{\rho_{qs}} \frac{d\rho_{qs}}{dt} = -\nabla \cdot \mathbf{v} + \epsilon,$$

$$\epsilon = \frac{(\kappa - 1)}{1 + q^x} \frac{dq^x}{dt},$$

$$\tilde{T} \equiv T(1 + q^x)^{-R/c_p},$$

$$q^x = (p - \pi)/\pi$$

Unified system – the non-linear equations

$$\frac{d\mathbf{v_h}}{dt} = -(1+q^x)^\kappa \left(1+\frac{\pi}{m(1+q^x)}\frac{\partial(1+q^x)}{\partial\eta}\right)(\nabla_\eta\phi) - R\tilde{T}(1+q^x)^{R/c_p}\left[\frac{\nabla_\eta\pi}{\pi}+\frac{\nabla_\eta(1+q^x)}{1+q^x}\right]$$

$$\frac{dw}{dt} = (1+q^x)^\kappa g\left[1+\frac{\pi}{m(1+q^x)}\frac{\partial(1+q^x)}{\partial\eta}-\frac{1}{(1+q^x)^\kappa}\right],$$

$$\frac{d\tilde{T}}{dt} = \frac{R\tilde{T}}{c_p}\left(\frac{\omega}{\pi}\right)+(1+q^x)^{-R/c_p}P_T,$$

$$\frac{d\pi_S}{dt} = \mathbf{v}\cdot\nabla\pi_S - \nabla\cdot\int_0^1 m\mathbf{v_h}d\eta + \int_0^1 \epsilon d\eta,$$

$$\frac{d\phi}{dt} = gw,$$

Unified system – the non-linear equations

$$
\begin{aligned}
\epsilon &= \frac{(\kappa - 1)}{1 + q^x}\frac{dq^x}{dt}, \\
\frac{1}{m}\frac{\partial\phi}{\partial\eta} &= -\frac{R\tilde{T}}{\pi}, \\
p &= \pi(1 + q^x), \\
\rho &= \rho_{qs}(1 + q^x)^{1-\kappa}, \\
m\dot{\eta} &= B\nabla_\eta \cdot \int_0^1 m\mathbf{v_h}d\eta - \nabla_\eta \cdot \int_0^\eta m\mathbf{v_h}d\eta + \int_0^\eta \epsilon d\eta, \\
\dot{\pi} &= \mathbf{v_h} \cdot \nabla_\eta\pi - \nabla_\eta \cdot \int_0^\eta m\mathbf{v_h}d\eta + \int_0^\eta \epsilon d\eta.
\end{aligned}
$$

Unified system – the linear system

$$\frac{\partial D'}{\partial t} = -\Delta\left[\gamma\tilde{T}' + RT^* q' + \frac{RT^*}{\pi_S^*}\pi'_S\right],$$

$$\frac{\partial w'}{\partial t} = g(\kappa + \partial^*)q',$$

$$\frac{\partial \tilde{T}'}{\partial t} = -\tau D',$$

$$\frac{\partial \phi'}{\partial t} = gw' - c_p\tau D' + RT^* B(\eta)\left(\frac{\pi_S^*}{\pi^*}\right)\nu D',$$

$$\frac{\partial \pi'_S}{\partial t} = -\pi_S^*\nu D',$$

Describes the small deviation from a hydrostatically balanced, isothermal, and resting reference state.

Unified system – the linear system

$$\frac{1}{H_*}\partial^* \left\{ \left[\Delta + \frac{1}{H_*^2}\partial^*(\partial^* + 1) \right] \frac{\partial^2}{\partial t^2} + N_*^2 \Delta \right\} w' = 0,$$

The structure equation is identical to the Lipps and Hemler system, or in other words, small perturbations from a hydrostatically balanced reference state show the *same behaviour in EULAG* and *the unified system* ! (in the absence of Coriolis at least.)

At large scales the unified system collapses to the existing hydrostatic system.

Semi-implicit schemes

linearised term, treated implicit

$$\frac{\delta \mathbf{X}}{\delta t} = (\mathbf{M} - \mathbf{L}^*) \cdot \mathbf{X} + \overline{\mathbf{L}^* \cdot \mathbf{X}}^t$$

non-linear term, treated explicit

SLSI solution procedure

$$X^{t+\Delta t,+} = X^{t,o} + \Delta t rhs^{t+0.5\Delta t,o,+} + \Delta t \left\{ -\beta \mathcal{B}^{t+0.5\Delta t,o,+} + 0.5\beta \mathcal{B}^{t,o} + 0.5\beta \mathcal{B}^{t+\Delta t,+} \right\},$$

$$\begin{aligned}
\tilde{T}_{t+\Delta t} &= \mathcal{T}^* - 0.5\beta\Delta t \tau D_{t+\Delta t}, \\
\log(\pi_S)_{t+\Delta t} &= \mathcal{P}^* - 0.5\beta\Delta t \nu D_{t+\Delta t}, \\
\phi_{t+\Delta t} &= \Phi^* + 0.5\beta\Delta t \left(g w_{t+\Delta t} - c_p \tau D_{t+\Delta t} + B \frac{\pi_S^*}{\pi^*} \mu \nu D_{t+\Delta t} \right), \\
w_{t+\Delta t} &= \mathcal{W}^* + 0.5\beta\Delta t g (\kappa + \partial^*) q^x_{t+\Delta t}, \\
D_{t+\Delta t} &= \mathcal{D}^* - 0.5\beta\Delta t \Delta \left(\gamma \tilde{T}_{t+\Delta t} + R T^* q^x_{t+\Delta t} + R T^* \log(\pi_S)_{t+\Delta t} \right)
\end{aligned}$$

Summary and outlook

- **"Pushing the boundaries" with first T_L3999 simulations.**
- **Nonhydrostatic IFS: Computational cost (almost 3 x at T_L3999) is a serious issue ! Even with the hydrostatic IFS at T_L3999 the spectral computations are about 50% of the total computing time.**
- **Fast Legendre Transform (*Tygert, 2008,2010)* shows some promise but to be evaluated further.**
- **Unified IFS hydrostatic-anelastic equations (*Arakawa and Konor, 2008*) (at least in the absence of Coriolis) have the same linear structure equation, i.e. show the same physical behaviour with respect to small perturbations as the Lipps/Hemler system in EULAG, while converging to the existing hydrostatic framework at hydrostatic scales !**
- **Possibilities in the framework of SLSI need to be explored !**

Additional slides

T1279 Skandinavia 24 h total cloud cover

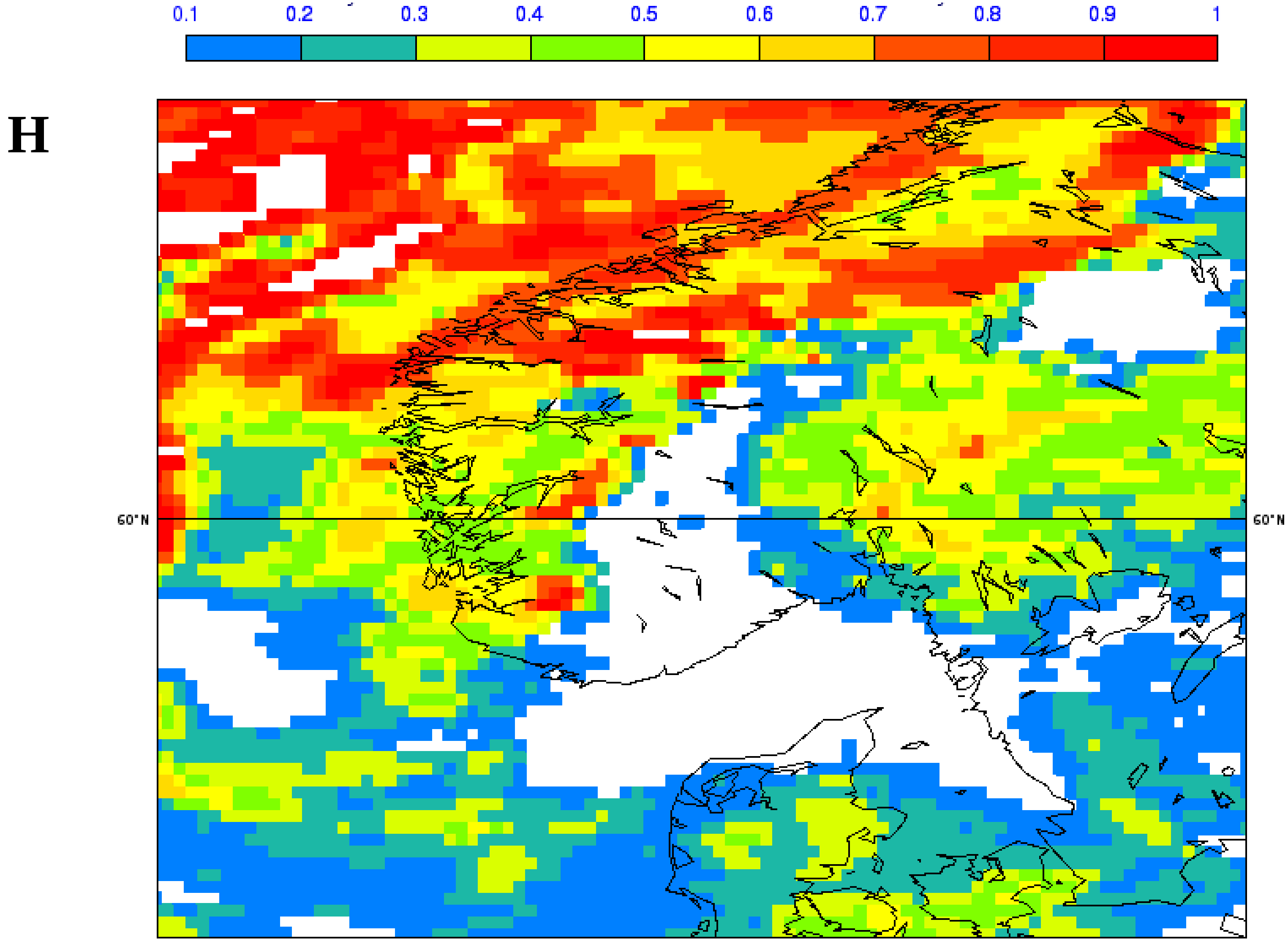

ECMWF

T3999 Skandinavia 24 h total cloud cover

H

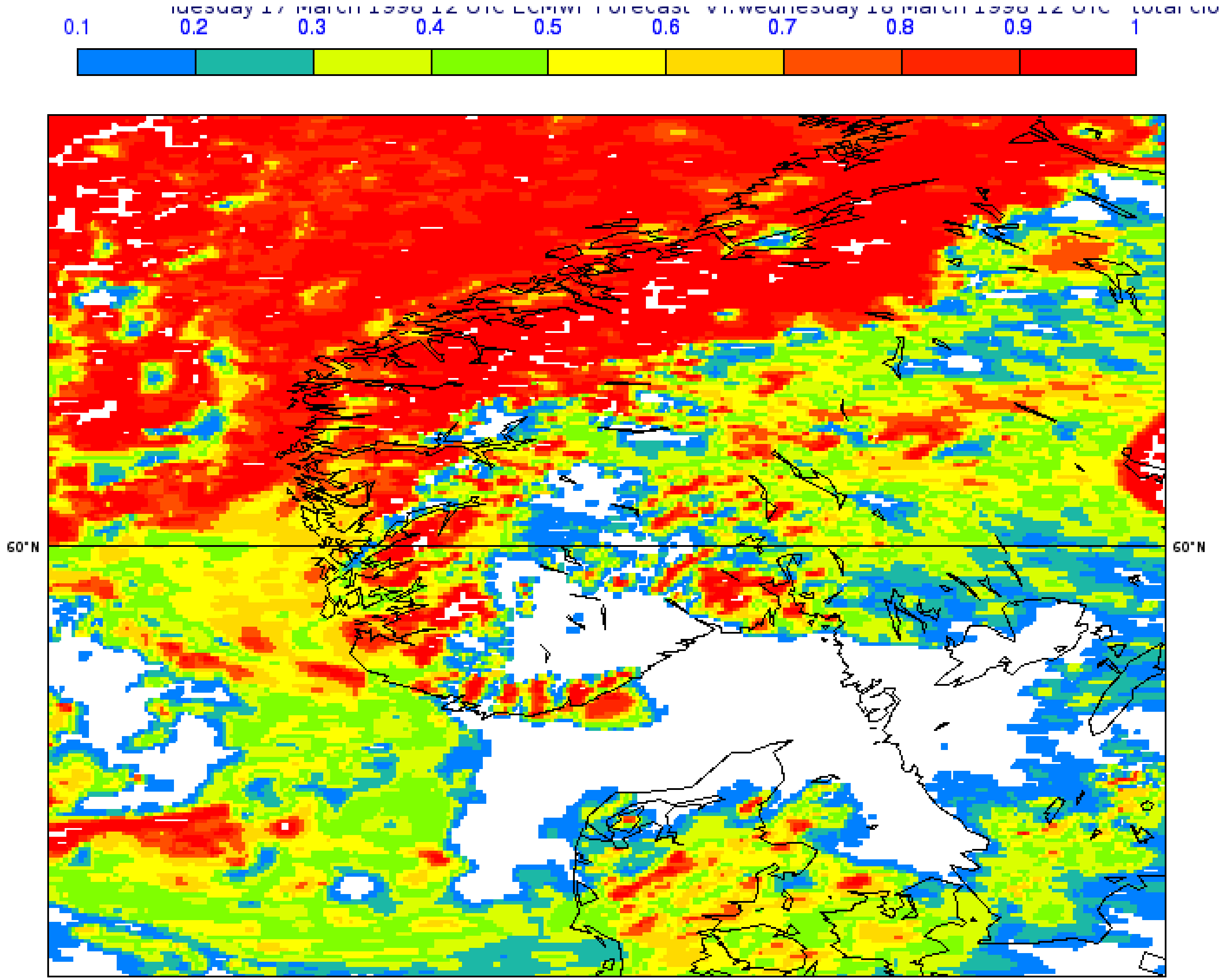

ECMWF

T3999 Skandinavia 24 h total cloud cover

NH

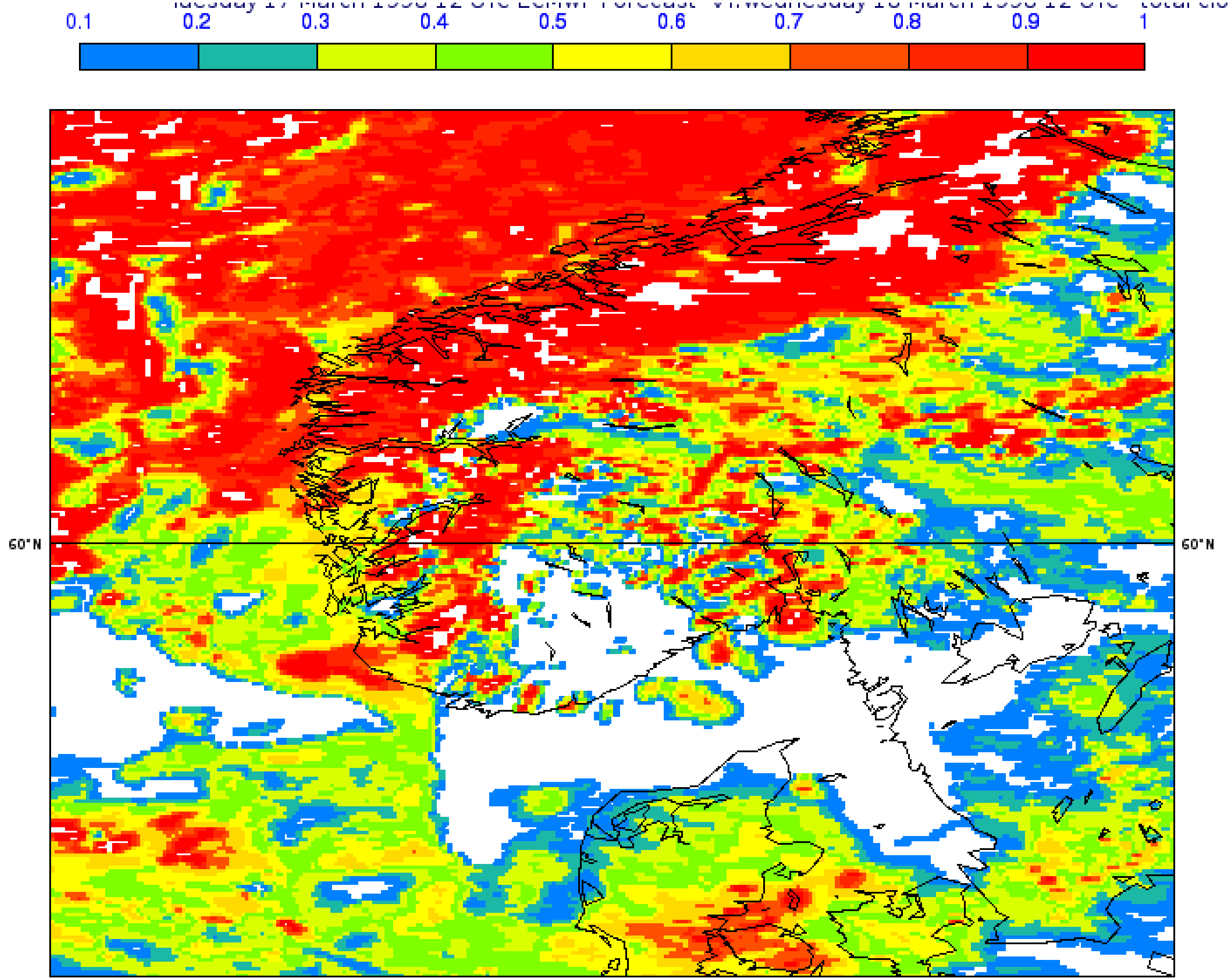

Unified system – linear system

$$
\begin{aligned}
\tilde{T} &= T^* + \tilde{T}', \\
\phi &= \phi^*(\eta) + \phi', \\
\phi_S &= 0, \\
\mathbf{v}_h &= \mathbf{v}_h', \\
D &= \nabla_\pi \cdot \mathbf{v}_h' = D', \\
w &= w', \\
q_0 &= q', \\
\pi &= \pi^*(\eta) + \pi', \\
\pi_S &= \pi_S^* + \pi_S', \\
\omega &= \omega',
\end{aligned}
$$